

Ultimate strength optimization of stiffened panels based on a meta-model for prediction by Artificial Neural Networks

João P. S. Lima¹, Paula C. Ornelas¹, Francisco Evangelista Junior¹

¹*Dept. of Civil and Environmental Engineering, University of Brasília, Brasília
Campus Darcy Ribeiro, 70910-900, Brasília, Brazil
joaoplima@ufg.br, paula.cid@aluno.unb.br, fejr@unb.br*

Abstract. To determine an optimum geometry of stiffened panels applied to hulls of ships about their ultimate strength (σ_{ult}), analyses are performed applying nonlinear FEM on stiffened panels subjected to axial load. A Artificial Neural Networks (ANN) metamodel is presented to predict responses demanding a smaller number of simulations by the nonlinear FEM to accurately assess the structural capacity. Initially a simply supported thin plate without stiffeners was adopted, called a reference plate, using its ultimate strength as a reference value for the study. A panel of volume $V_r=91.035 \times 10^6 \text{ mm}^3$ was adopted. After that, part of its volume has been converted into stiffeners, which were incorporated into the plate, without varying the final volume of the plate. This made it possible to evaluate the design variables plate thickness (t_p), as well as the ratio between the height of the stiffener and its thickness (h_s/t_s). In response, the use of Cross-Entropy (CE) optimization algorithm and the ANN to predict a sampling by Monte Carlo allowed an optimization of the design variables resulting in a stiffened plate model with approximately 3.5 times resistance of a plate of the same volume, length, and width, but without stiffeners.

Keywords: Artificial Neural Networks; Finite element analysis; Ultimate strength optimization.

1 Introduction

Stiffened plates are one of the basic components in ships' hulls structures and, due to their thin-walled nature, are susceptible to post-buckling deformation because of an increased load. This behavior represents an important safety margin for board design (Gambhir [1]). Furthermore, in a wave condition, the elements present in the lower and lateral part of the hull are subjected to uniaxial and biaxial compressive loads (Xu *et al.* [2]).

According to Cai *et al.* [3] the stiffened plates optimization process deals with shape optimization with variable topology, as a result, it is important to design the structural members optimally, choosing the optimal geometric dimensions of the plate, as well as the excellent geometric relationships for the stiffeners to be applied. Therefore, realizing a structural optimization analysis will idealize optimal structural performance. Moreover, according to Chojaczyk *et al.* [4] sampling simulation techniques have their origin in the Monte Carlo (MC) simulation method, which generates randomly a large set of samples. Therefore, in optimization problems, large sample numbers of numerical analysis can favor prohibitive computational efforts. Thus, to overcome the high computational demand the use of metamodels for the limit state functions can be considered to provide accurate approximations at a low computational cost (Gaspar *et al.* [5]). In addition, the parameters that define the optimization variables are usually obtained by several tests, but these tests are expensive and time-consuming. Studies such as Borges *et al.* [6] present numerical evaluations of the limit state of structures.

As a surrogate solution, Machine Learning (ML) metamodels can be used as prediction models (Nguyen *et al.* [7]). Also, according to the authors, the most significant advantage of ML models is certainly dealing with non-linear input-output relationships, which are not easily expressed in mathematical models considering the variables they involve. The Artificial Neural Networks (ANNs), model based on ML, has been applied to several engineering problems. For example, Zhu, et al. [8], Chojaczyk *et al.* [4] and, Nguyen *et al.* [7].

Therefore, the present study will perform a numerical analysis of the mechanical behavior of plates with flat-bar stiffeners through the non-linear Finite Element Method (FEM) to determine, using Cross-Entropy (CE) algorithm, its optimized geometric configuration that leads to the best ultimate strength performance subject to axial compression. A prediction and metamodel based on Artificial Neural Networks (ANN) is presented.

2 Stiffened panel structural model

As fundamental models, stiffened panels proposed by Tanaka *et al.* [9], from the bottom plating of the bulk carrier are selected. The schematic illustration of the model is shown in Fig. 1. As shown in Fig.1, the square plate has the main dimension as $B=2550$ mm, and t_p is a thickness of the local panel partitioned by stiffeners. The spacing between adjacent longitudinal stiffeners is denoted as b , defining an aspect ratio of the local panel taken as $B/b = 3.0$. The stiffened panel is composed of two longitudinal stiffeners equally spaced with a Flat-type cross-section with h_s being the height and t_s the thickness of the stiffeners. In the present study, the degrees of freedom are represented by the ratio of the height/thickness dimensions of the stiffeners (h_s/t_s) and t_p . The material adopted in this study is the AH-36 steel with yield stress: $\sigma_y=355$ N/mm²; Young's modulus: $E=210000$ N/mm², and Poisson's ratio: $\nu=0.3$.

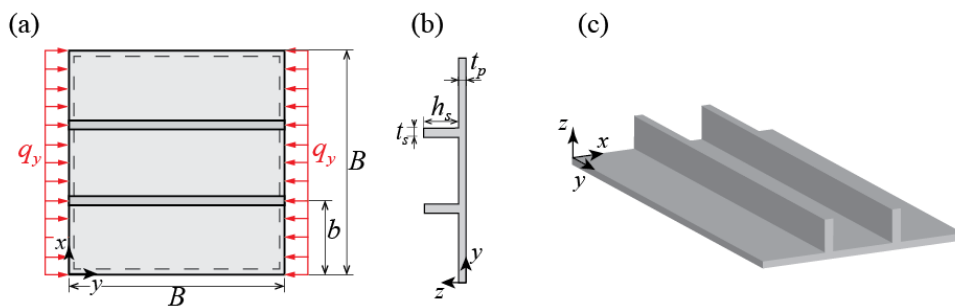


Figure 1. Stiffened plate model for bulk carriers. (a) top, (b) lateral and (c) isometric views

In the proposed model, longitudinal girders and transverse frames are provided on plating, for that reason, a panel with the four edges simply supported along the lines of its fixation is assumed. All nodes along the four edges are constrained to deflection and rotation along the thickness direction ($u_z, r_z=0$). The two unloaded edges are constrained with $u_y=0$, making them deform in the plane, but with the displacements being uniform along the length of the plate. The reactive edge is constrained to axial deformation at $u_x = 0$. A load q_y is applied axially on the two perpendicular edges (along x).

2.1 Nonlinear FEM analyses on stiffened panels

For the present study, the structural behavior of a set of stiffened plates under uniaxial compression is computed through nonlinear FE analysis using the ANSYS software. To do so, the SHELL93 finite element was adopted once it was already used satisfactorily in similar previous works (Lima, *et al.* [10], Lima, *et al.* [11]). The SHELL93 is a quadrilateral isoparametric finite element, having eight nodes with six degrees of freedom per node: rotations around the x , y , and z axes, and three translations in the x , y , and z directions. The finite element mesh is generated considering a quadratic element with side $l=50$ mm. It is important to emphasize that both the plate and the stiffeners have the same element size. The nonlinear material behavior is modeled using a linear-elastic and ideally-plastic material law, neglecting the strain hardening effect.

The structural analysis will be done as proposed by Paik, *et al.* [12]. According to the authors, this analysis is related to use geometric nonlinearity associated with buckling and material nonlinearity due to yielding or plastic deformation. So, a buckling eigenvalue analysis using FEM is performed, thus discovering the buckling mode of the plate. In the next step, the buckling mode obtained through the eigenvalue analysis is amplified to configure the maximum initial imperfection of the plate corresponding to a value of $w_0=b/200$ (Paik, *et al.* [12]).

For the analysis of the plate's ultimate load, according to Lima, *et al.* [11], a reference load is given by

$P_y = \sigma_y t_p$, applied in small increments to the edges parallel to the y axis of the plate (Fig. 1). In each load increment, the Newton-Raphson method is applied to determine the displacements corresponding to the equilibrium configuration of the plate.

3 A proposed approach using Artificial Neural Networks

In the ANN, the neuron is a processing element with several inputs and one output. In this present study the multi-layer feed-forward perceptron (MLP), will be trained by using the data (Chojaczyk *et al.* [4], Nguyen *et al.* [7]). In the MLP algorithm the neurons are classified into three components: (i) input layer, where enter input parameters, (ii) one or more hidden layers, and (iii) an output layer, which contains the expected result. Fig. 3 depicts an ANN model.

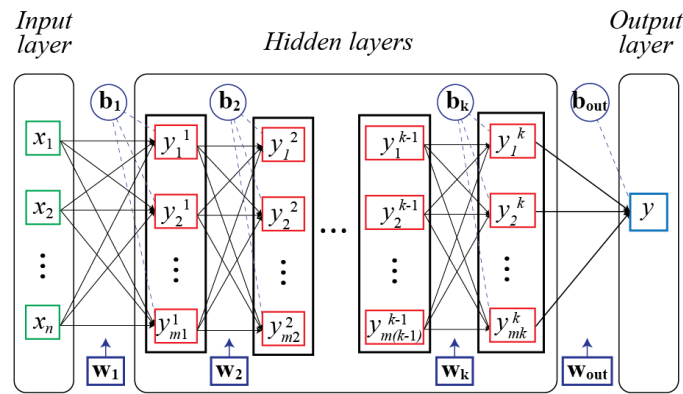


Figure 2. Depiction of the proposed ANN model

Fig. 2 shows that the number of neurons in the input layer is equivalent to the number of input variables, while in the output layer it depends on the number of outputs to be approximated. However, the selection of network optimal architecture is not a simple task, and no general rules are apposite for the number of hidden layers and the number of neurons in the hidden layer estimations (Chojaczyk *et al.* [4], Nguyen *et al.* [7]). Fig. 3 illustrates m as the number of neurons. Each neuron receives an input signal vector $\mathbf{x}=[x_1, x_2, \dots, x_n]$ from n input channels. These neurons are connected, in which the connection has a weight w , and each neuron contains a bias and an activation. Next, the weighted sum of x is calculated by multiplying each element x_k by a coefficient w_{mk} demonstrating the proper importance of input channel k . The activation a_m of the m -neuron is:

$$a_m = \sum_{k=1}^n w_{mk} x_n + b_m \quad (1)$$

where $b_m \in R$ is the bias, is a constant corrective term which allows having a non-negative activation a_m when all elements of the input vector \mathbf{x} are $\mathbf{0}$. The output signal value y is calculated as a function of the activation. It is necessary to perform non-linear processing in a_m to represent the non-linear relationship between the input and output layers. The Rectified Linear Unit (relu) functions were used.

However, scaling is necessary because differences between two values that are too high or too low will result in an insignificant difference in function output, which makes the training process difficult (Iman *et al.* [13], Nguyen *et al.* [7]). To start the training process, training data need to be scaled, so that $x_i \in [0,1]$, before introducing to the network. In the feed-forward back-propagation algorithm, the input data are provided to the input layer, which transfers the information forward, through the different connections, from one neuron to another in the network. The Adam algorithm was adopted to adjust the ANN model weights and biases. This is a method for efficient stochastic optimization that only requires first-order gradients with little memory requirement, is uncomplicated to implement, computationally efficient, and is well suited for problems that are large in terms of data and/or parameters (Kingma and Ba 2017 [14]). Since the output from the forward pass is obtained, the default error function used for training feed-forward networks is the mean squared error (MSE). To find the optimal weights and biases that can minimize the MSE, expressed as:

$$MSE = \frac{1}{N} \sum_{i=1}^N p_i - t_i^2 \quad (2)$$

where N is the number of samples, t_i and p_i are the target and predicted values of the i^{th} sample, respectively.

In general, the higher the complexity of a problem, the larger the number of processing elements in the hidden layer is needed for a good approximation level, and often this is found based on a trial-and-error process. In this study, the trial-and-error method was used to obtain the number of hidden layers as well as the number of neurons in each hidden layer. The number of neurons is decided by the input and output parameters. All analyzes were performed using Keras and TensorFlow package in Python language.

For this present study, 135 samples were considered. The sample data are taken of another analyzes. All samples have constant total volume $V_f=91.035 \cdot 10^6 \text{ mm}^3$. This volume refers to a plate with the same dimension B proposed, but without the presence of stiffeners and with plate thickness $t_p=14 \text{ mm}$. Keeping the value of B fixed, a volumetric fraction of the material will be transformed into stiffeners, as shown in Fig. 1. In this way, there is a variation of the input variables of the ANN h_s/t_s and t_p . The sample plan was distributed along with the two variables as shown in Fig. 3. For each sample, a numerical simulation was performed in the Ansys software.

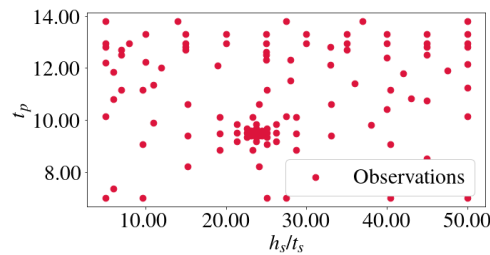


Figure 3. Sample data

The combinatorial optimization problem resulted from the FEM formulation is solved by an algorithm based on the CE method. The CE algorithm is a stochastic optimization method based on the probability model proposed by Rubinstein [16]. It consists of an adaptive importance sampling method that can be used to search for improved solutions of optimization problems. The CE algorithm has a statistical theoretical foundation, and the Monte Carlo (MC) method is used to estimate the high-dimensional integrals in the parameter update. So that its effectiveness, according to Rubinstein [16] depends on the construction of the probability model and parameter updating to ensure the estimation accuracy. To apply the CE optimization let X be an arbitrary set of states and S a real-valued performance function on X . The goal is to maximize S over X , and the corresponding optimum \mathbf{x} . Denote the maximum by γ^* , so that:

$$S \mathbf{x}^* = \gamma^* = \max_{\mathbf{x} \in X} S \mathbf{x} . \quad (3)$$

Step 1: Input initial statistical vector \mathbf{v}_0 , sample size N . and rarity parameter ρ . Let $N_e=\rho N$ (number of elite samples) and set $t = 1$ (level counter).

Step 2: Generate $\mathbf{X}_1, \dots, \mathbf{X}_N \sim \text{iid} f(\cdot, \mathbf{v}_{t-1})$, where $\mathbf{X}_1, \dots, \mathbf{X}_N$ are iid samples. Compute $S(\mathbf{X}_i)$ for all i , and order them from smallest to largest: $S_{(1)} \leq \dots \leq S_{(N)}$. Let γ_t be the sample ρ -quantile of performances; that is, $\gamma_t = S_{(N_e)}$.

Step 3: Use the same sample $\mathbf{X}_1, \dots, \mathbf{X}_N$ and solve the stochastic program:

$$\max_{\mathbf{v}} \sum_{k=1}^N \mathbf{I} S \mathbf{X}_k \leq \gamma_t \ln f \mathbf{X}_k; \mathbf{v} . \quad (4)$$

Step 4: While the sampling distribution is not degenerate, denote the solution by \mathbf{v}_t , set $t=t+1$ and go to Step 2.

4 Results

Using as a reference the ultimate strength of the plate with the same volume $V_f=91.035 \cdot 10^6 \text{ mm}^3$, but without stiffeners ($\sigma_{uR}=63.950 \text{ N/mm}^2$), the ultimate strength values for the cases of plates with stiffeners were

normalized, obtaining the values σ_{uN} .

4.1 Computational Model Verification

The verification of the computational model of elastoplastic buckling was performed considering a plate with longitudinal T-section stiffeners under axial compression proposed by Estefen, *et al.* [14]. In the structure $a=200$ mm, $b=185,39$ mm, $t_p=1,03$ mm, $h_s=22,6$ mm, $t_s=0,77$ mm, $t_f=1,03$ mm, $c_1=18$ mm and $c_2=36$ mm. The material properties used are $\sigma_Y=381.4$ N/mm², $E=207800$ N/mm², and $\nu=0.3$. The edges on which the axial load is applied were considered clamped (one of them has the allowable translational movement in the y-direction) while the other edges were considered simply supported. The initial imperfections for the models presented were mapped with sub-millimeter precision equipment. For the numerical analysis, the authors adopted the ABAQUS FE software, and the discretization was performed with the shells4R element. To verify the computational model, the same mesh discretization was proposed by Estefen, *et al.* [15], however, with the finite elements SHELL93 of ANSYS software. According to Estefen, *et al.* [14], the Ultimate Axial Force (F_{ult}) values of 142,506 kN and 134,347 kN were obtained for the experimental and numerical analyzes of the stiffened panel under axial compression. In the numerical analysis in the present study, $F_{ult} = 131.797$ kN was obtained. This value presents a difference of 7.515% and 1.898% concerning the experimental and numerical results obtained by the model proposed by Estefen, *et al.* [15]. From the F_{ult} results, a good agreement can be seen between the numerical and experimental results obtained by Estefen, *et al.* [15], when compared to the proposed model.

4.2 The ANN prediction model

The ANN model for ultimate strength response prediction consists of a prediction model where four hidden layers were considered. The neurons in the input layer represent the two input parameters (t_p and h_s/t_s). Through a sensitivity analysis, 256 neurons were adopted in the first hidden layer and 128 in others. The neuron in the output layer refers to the value of the ultimate buckling strength of the plate (σ_{ult}). In the layers of this network, the relu activation function was used. The model will be evaluated over 100 epochs and a fraction of 33% of the training data was randomly selected to be used as test data. To analyze the results of trained ANN, the coefficient of determination (R^2) can be applied as an adjustment indicator to measure the variation between predicted and actual data. Fig. 4 compares the application of a simple linear regression with a trained ANN.

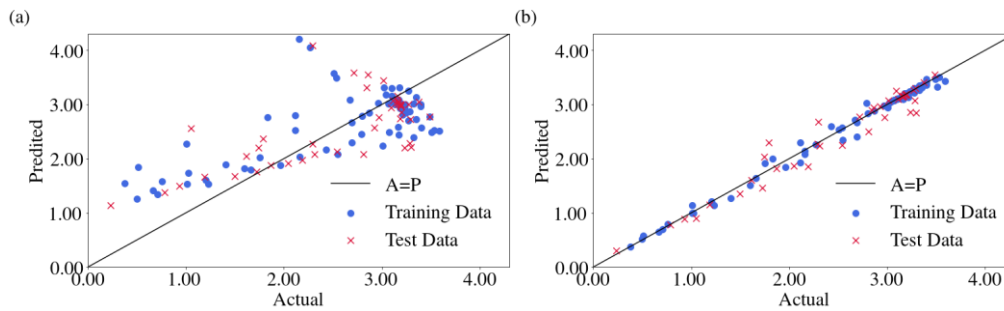


Figure 4. Comparison between actual and predicted σ_{uN} by (a) Linear regression (b) ANN.

Fig. 4a shows the relationship between the actual values and the predicted results obtained by a simple linear regression considering the sample points. For this analysis, a coefficient of determination $R^2= 0.529$ and 0.492 was obtained for the training and test samples, respectively. This value can be compared to that of an ANN used as a prediction ANN model (Fig. 4b), obtaining $R^2= 0.991$ and 0.953 for the training and test samples, respectively. This comparison once again underscores the feasibility of the proposed ANN model. The model also was evaluated through the MSE metric on that data at the end of each epoch. Fig. 5a shows the performance of the ANN model developed for the prediction model over 100 epochs. For each epoch, the MSEs for training and testing were obtained as a response. In general, the system enters convergence over the analyzed periods. Fig. 5b zooms in and details the MSE curves by epoch indicating a value of 0.0058 for the MSE of the training samples and 0.0317 for the test samples in the established stopping criterion (100 epochs). The low MSE values found imply that the ANN model was well trained.

Finally, with trained and tested ANN, it is possible to remove the computational cost calculation barrier to solving optimization problems in cases where the use of linear regression is not feasible. In this way, it is possible to carry out the association of the trained neural network to perform the analysis of the optimal ultimate normalized strength value (σ_{uN}^{opt}). This value will be associated with the optimal combination of t_p^{opt} e $(h_s/t_s)^{opt}$.

An analysis using trained ANN is proposed generating a MC sampling analysis to determine σ_{uN}^{opt} . A sample group of $N=10^5$ observations will be analyzed. For this analysis, it was possible to determine the case that guarantees a performance with σ_{uN}^{opt} .

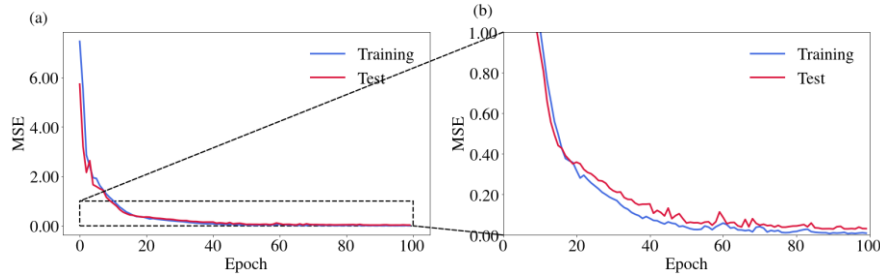


Figure 5. MSE values for Training and Test points for trained ANN

For uncertainty quantification in the present case the MC sampling was used. Fig. 6a shows the σ_{uN} histogram for the sample group with $N=10^5$ under investigation. As shown in the horizontal axis, a variation in the range of σ_{uN} values in the sample space can be evaluated. The σ_{uN} values have a mean $\mu=2.632$, and standard deviation $sd=0.7600$. However, through the optimization process, σ_{uN} values greater than average μ are observed.

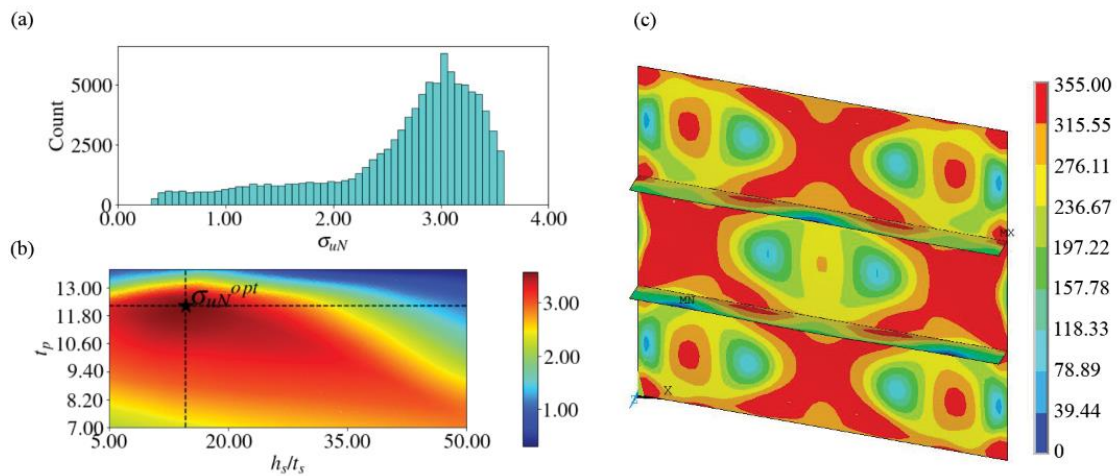


Figure 6. MC data sample results (a) Histogram of predicted values of σ_{uN} , ANN predictions of σ_{uN} . (b) Effect of $(h_s/t_s) \times t_p$ over σ_{uN} ; (c) Distribution of the von Mises stress for optimized geometry.

Fig. 6b presents a heat map to represent the ANN predictions of σ_{uN} for the different sample sizes presented. By MC analysis, the optimal sampling point with $(h_s/t_s)^{opt}=14.057$, $t_p^{opt}=12.106$ resulting in $\sigma_{uN}^{opt}=3.578$. Fig. 6c depicted the tension distribution for the optimal sampling point. Examining Fig. 6c, it is possible to observe the stress distribution for the optimal sampling point. It is observed that the von Mises stress distributions on the plates follow the local deformations caused by the axial compression resulting in three semi-waves in the plates placed between the stiffeners.

5 Conclusions

The ANN metamodel for the stiffened plates system presented an optimization of the design variables with

the objective function of maximizing the σ_{ult} of the plates with the presence of the stiffeners through an analysis that reduced the computation cost in the optimization process. This shows the importance of studies that combine the ability to reduce time and computational cost, showing satisfactory results in structural optimization. Moreover, the study enabled an analysis of the design variables, allowing the evaluation of the relationship between plate thickness (t_p) and the height/thickness characteristics of the stiffener (h_s/t_s) with the ultimate strength of the stiffened plate.

For the proposed analysis, using CE-MC optimization process, allows finding a optimal performance observed in the stiffened plate whose $t_p^{opt}=12.106$ and $(h_s/t_s)^{opt}=14.057$, presenting an improvement of $\sigma_{uN}^{opt}=3.578$, upon for the plate with the same initial volume of material, but without stiffeners. This gain points to the importance of studying the optimization of these structural elements and serves as an initial research analysis, which can be expanded in future work by applying the ANN models for other purposes such as creating classification systems by type of buckling, overall or local, analyze other models of stiffened plates with different purposes, as well as the study of different metamodels to analyze independent variables which directly influence the design of stiffened plates.

The results obtained show that ANN methodologies are robust and efficient alternatives to traditional optimization methods for the analysis of complex structures and sets the base for future research developments considering uncertainty quantification and reliability analysis.

References

- [1] M. Gambhir. *Stability Analysis and Design of Structures*. Springer-Verlag Berlin Heidelberg, 2004
- [2] M. C. Xu, Z. J. Song, J. Pan and C. G. Soares. "Ultimate strength assessment of continuous stiffened panels under combined longitudinal compressive load and lateral pressure." *Ocean Engineering*, vol. 139, pp 39-53, 2017.
- [3] S. Cai, W. Zhang, J. Zhu and T. Gao. Stress constrained shape and topology optimization with fixed mesh: A B-spline finite cell method combined with level set function." *Computer Methods in Applied Mechanics and Engineering*, vol. 278, pp. 361-387, 2014.
- [4] A. A Chojaczyk, A. P. Teixeira, L. C. Neves, J. B. Cardoso and C. Guedes Soares. "Review and application of Artificial Neural Networks models in reliability analysis of steel structures." *Structural Safety* vol. 52, pp. 78-89, 2015.
- [5] B. Gaspar, A. P. Teixeira and C. Guedes Soares. "Adaptive surrogate model with active refinement combining Kriging and a trust region method." *Reliability Engineering & System Safety*, vol. 165, pp.277-291, 2017.
- [6] J. F. Borges, V. F. de Paula, F. Evangelista and L. M. Bezerra. "Reliability and uncertainty quantification of the net section tension capacity of cold-formed steel angles with bolted connections considering shear lag." *Advances in Structural Engineering*, vol. 24, is. 1, 2020.
- [7] D. D. Nguyen, V. L. Tran, D. H. Ha, V. Q. Nguyen and T.H. Lee. "A machine learning-based formulation for predicting shear capacity of squat flanged RC walls." *Structures*, vol.29, p.p. 1734-1747, 2021.
- [8] S. Zhu, M. Ohsaki and X. Guo. "Prediction of non-linear buckling load of imperfect reticulated shell using modified consistent imperfection and machine learning." *Engineering Structures*, vol. 226, 2021
- [9] S. Tanaka, D. Yanagihara, A. Yasuoka, M. Harada, S. Okazawa, M. Fujikubo and T. Yao. "Evaluation of ultimate strength of stiffened panels under longitudinal thrust." *Marine Structures*, vol. 36, pp. 21-50, 2014.
- [10] J. P. S. Lima, M. L. Cunha, E. D. dos Santos, L. A. O. Rocha, M. d. V. Real and L. A. Isoldi. "Constructal Design for the ultimate buckling stress improvement of stiffened plates submitted to uniaxial compressive load." *Engineering Structures* vol. 203, 2020.
- [11] J. P. S. Lima, L. A. O. Rocha, E. D. dos Santos, M. d. V. Real and L. A. Isoldi (2018). "Constructal design and numerical modeling applied to stiffened steel plates submitted to elasto-plastic buckling." *Proceedings of the romanian academy, series a*, Special Issue: pp.195-200, 2018.
- [12] J. K. Paik, B. J. Kim and J. K. Seo. "Methods for ultimate limit state assessment of ships and ship-shaped offshore structures: Part II stiffened panels." *Ocean Engineering*, vol. 35(2), pp. 271-280, 2008.
- [13] M. N. Iman, R. R. Saman and A. Hamed. "A new empirical formula for prediction of fracture energy of concrete based on the artificial neural network." *Engineering Fracture Mechanics*, vol. 186, pp. 466-482, 2017.
- [14] D. P. Kingma, J. L. Ba. Adam: A method for stochastic optimization. *International Conference on Learning Representations 2015*, 2017
- [15] S. F. Estefen, J. H. Chujutalli and C. Guedes Soares. "Influence of geometric imperfections on the ultimate strength of the double bottom of a Suezmax tanker.", *Engineering Structures*, vol. 127, pp. 287-303, 2016.
- [15] R.Y. Rubinstein. "Optimization of computer simulation models with rare events.", *Eur. J. Oper. Res*, vol. 99, pp. 89-112, 1997.

Authorship statement. The authors hereby confirm that they are the sole liable persons responsible for the authorship of this work, and that all material that has been herein included as part of the present paper is either the property (and authorship) of the authors or has the permission of the owners to be included here.